Charge front and negative differential mobility in HVDC model cables

T. T. N. Vu, Gilbert Teyssedre, B. Vissouvanadin, Christian Laurent

Charge front and negative differential mobility in HVDC model cables

Thi Thu Nga Vu[1,2], Gilbert Teyssedre[1*], Bertrand Vissouvanadin[1], Christian Laurent[1]
LAPLACE (Laboratoire Plasma et Conversion d'Energie), Université de Toulouse; CNRS, UPS, INPT;
118 route de Narbonne, F-31062 Toulouse cedex 9, France
*Corresponding author: gilbert.teyssedre@laplace.univ-tlse.fr

***Abstract*— Space charge measurements have been carried out by means of pulsed-electro-acoustic (PEA) method on mini-cables with 1.5 mm-thick cross-linked polyethylene (XLPE) as insulation. Measurements were realized at room temperature or with a temperature gradient of 10°C through the insulation (T_{in} = 70°C, T_{ext} = 60°C) under DC voltage of -30kV and -55kV. Space charge results highlight the enhancement of the field at the outer-electrode when combining thermal and electrical stresses. They also reveal systematic occurrence of a negative front of charges generated at the inner electrode that moves toward the outer electrode at the beginning of the polarization step. It is observed that the transit time of the front of negative charge increases, and therefore the mobility decreases, with the applied voltage. Further, the estimated mobility –in the range 10^{-14} – 10^{-13} $m^2V^{-1}s^{-1}$ for the present results, increases when the temperature increases for the same condition of applied voltage. The possible origin of this charge front is discussed on the basis of transient charging current measurements realized on the same cables. The features substantiate the hypothesis of negative differential mobility used for modelling space charge packets.**

Keywords—space charge, HVDC, model cable, charge injection, negative differential mobility.

I. INTRODUCTION

The recent impulse in demand for HVDC cable systems, owing e.g. to the need for higher transmission capacity in applications such as integration of wind power and more interconnected power networks, has reactivated researches on extruded insulations for cables, with new generations of crosslinked polyethylene grade and understanding of space charge features in such cables as main concerns. Because of the nonlinearity of conduction processes in these materials and substantial temperature dependency of conductivity the prediction of field distribution as a function of stressing conditions remains a hazardous exercise. For these reasons, space charge measurements on cable models remain an essential task. In these measurements, space charge features in polyethylene materials have revealed various forms of instability as for example 'slow' charge packets with mobility in the range 10^{-14} – 10^{-16} $m^2V^{-1}s^{-1}$ observed repetitively under relatively high fields (100kV/mm or so) [1], or 'fast' charge packets with a much higher mobility of the order of 10^{-10} $m^2V^{-1}s^{-1}$ reported more recently and more seldom [2].

Slow charge packets have been reported for many years, both in thick insulations as in cables [3], or in flat specimen [4]. The repetitive nature of the process is one of the characteristics of charge packets and also one of the challenges when attempting to model the phenomenon [5]. So called fast-packets tend to be transient phenomena with very small amount of charge quantity being transported. They were detected under moderate stress, pointing towards harmfulness of the process under DC service field [6]. In this communication, we report on a specific kind of charge front with an intermediate mobility observed in HVDC miniature cables and featuring an apparent decrease of the mobility of the charge front with increasing the applied voltage.

II. EXPERIMENTAL SECTION

A. Samples

Samples used for conductivity and space charge measurements are crosslinked polyethylene-insulated –XLPE- miniature cables provided by Nexans. The test samples are sections of cables of approximately 3 m in length. The insulation thickness is 1.5 mm; the other characteristic dimensions are reported in Fig. 1. Samples were outgassed prior to measurements in order to remove volatile by-products.

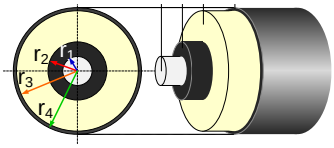

Fig. 1: Section of mini-cable samples. Inner conductor radius r_1=0.7 mm; Inner semi-conductor radius r_2=1.4 mm; Insulation radius r_3=2.9 mm; Outer semi-conductor radius r_4=3.05 mm.

B. Space charge and current measurements on mini-cable samples

Space charge measurements have been carried out using the pulsed electro-acoustic (PEA) method through the configuration of Fig.2. The PEA cable device was provided by TechImp S.p.A., Italy. The cable was fixed to the PEA cell using a mechanical holder insuring a good acoustic contact between the outer SC and aluminum electrode of the measuring device.

A pulse generator, specified with 30ns voltage pulse half-width, up to 5 kV amplitude and up to 10 kHz repetition rate, was used as excitation source. The pulses were injected via the outer SC of the cable. The outer SC was removed over a length

Cite as: T.T.N. Vu, G. Teyssedre, B. Vissouvanadin, C. Laurent, "*Charge front and negative differential mobility in HVDC model cables*", IEEE Int. Conf. on Electrical Insulation and Dielectric Phenomena (CEIDP), Ann Arbor, MI, USA, 18-21 Oct. 2015. Proc. CEIDP, pp. 19-22, **2015**. DOI: 10.1109/CEIDP.2015.7352104

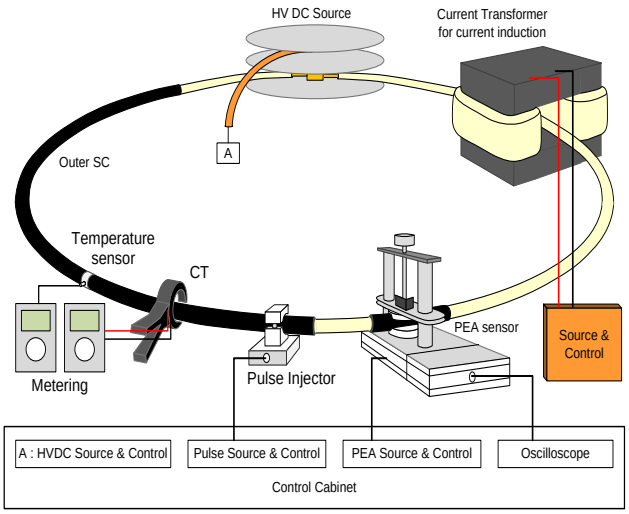

Fig. 2: Schematic representation of the PEA Cable system

of 5 cm (cf. Fig. 2) between the measuring location and the region where pulses are applied creating a decoupling capacitor between pulse and HVDC supply. For electrical stress, a negative DC voltage was applied to the cable conductor. Two voltage levels were investigated in this work: -30 kV and -55 kV, providing Laplace fields E_I of ~ -30 kV/mm and -55 kV/mm at the interface with the inner SC, respectively; and -14 kV/mm and -26 kV/mm at the outer SC.

Space charge measurements were performed under two different temperature conditions: at room temperature (~22°C) and under a temperature gradient through the cable radius. To achieve a temperature gradient across the cable insulation, a current was injected into the cable core by means of a current transformer, as shown in Fig. 2, while the external surface of the semiconductor was kept in ambient. For the latter condition, the targeted temperature at the inner semiconducting screen was 70°C. Thermal modelling of the cable was achieved to set the current to be injected targeting a temperature of 70°C at the inner SC. The result was a current of 32 A, providing a surface temperature of the cable of 60°C.

The amplitude of pulses in the PEA measurement was set to 400 V and repetition frequency to 5 kHz. PEA measurements consisted in a cycle of 4h/4h of polarization/depolarization. One new cable sample was used for every stress level. Space charge profiles were recorded every 200 seconds throughout the measurement protocol. The calibration procedure used for space charge recovery is described in [7].

Current measurements were realized on mini-cable samples. The outer SC was removed in some section of the cable for preventing surface conduction. Guard electrodes of 1cm width were created at both ends of the active area of measurement by removing the outer SC. The measuring electrode of 20 cm length, 1 cm apart from the guard electrodes, was connected to a Keithley 617 electrometer through a protecting circuit. The cable sample was placed in an oven in air at atmospheric pressure for controlling the temperature. Measurements were performed under different temperatures varying from 30°C to +90°C by step of 10°C. For each of the temperature levels, charging/discharging current measurements were realized for 10 values of applied field ranging between 2 and 25 kV/mm under isothermal conditions. Polarization/depolarization steps last for 1h/1h. A new sample has been used for each value of temperature to avoid possible memory effects. Current values were recorded every 2 seconds all along the measurements.

III. RESULTS AND DISCUSSION

A. *Space charge patterns*

Fig.3 shows typical space charge patterns obtained under the different conditions of temperature and stress that have been investigated. Two phenomena are worth mentioning here. On the one hand, negative charges appear to be dominant carriers in the patterns, and appear to be formed from injection from the cathode, i.e. the inner conductor in experiments. The second feature is a front of charges developing upon injection at the cathode and crossing the insulation. The front appears relatively narrow all along its travel through the insulation.

1) *Bulk space charge due to conductivity gradient.*

Let us consider first the negative charge build-up in the bulk of the insulation and consider what is expected as charge distribution due to non-homogeneous field situation using Maxwell's equation. In cylindrical geometry, in the hypothesis of a radius dependence of the electrical conductivity, it can be deduced considering the conservation of the current that the electric field distribution in the cable insulation, under steady state condition is given by [8]:

$$E(r) = E_0 \frac{r_0 \sigma_0}{r\sigma(r)} \quad (1)$$

where E_0 and σ_0 are respectively the electric field and conductivity at the reference position r_0. Considering the Poisson's equation:

$$\mathrm{div}E = \frac{\rho}{\varepsilon} \quad (2)$$

where ε is the dielectric permittivity of the material, it can readily be deduced that the space charge distribution associated to a non-uniform conductivity along the radius is of the form:

$$\rho(r) = -E(r)\frac{\varepsilon}{\sigma(r)}\frac{d\sigma(r)}{dr} \quad (3)$$

The conductivity gradient may have several origins in the context of XLPE cables:

(i) a non-linear field dependence of conductivity associated with the radial dependence of the field;

(ii) a thermal gradient along the cable radius when energizing the cable, with inner interface temperature larger than outer temperature;

(iii) a gradient in the material properties, with e.g. crosslinking by-products concentration gradient as reported e.g. by Jeroense et al. [9].

Except for the last instance where the nature of material changes and its impact on conductivity has to be anticipated, the sign of the space charge can be easily predicted. Field gradient induced space charge and thermal gradient normally lead to decrease of the conductivity with the radius. Therefore, as by

Cite as: T.T.N. Vu, G. Teyssedre, B. Vissouvanadin, C. Laurent, "*Charge front and negative differential mobility in HVDC model cables*", IEEE Int. Conf. on Electrical Insulation and Dielectric Phenomena (CEIDP), Ann Arbor, MI, USA, 18-21 Oct. 2015. Proc. CEIDP, pp. 19-22, **2015**. DOI: 10.1109/CEIDP.2015.7352104

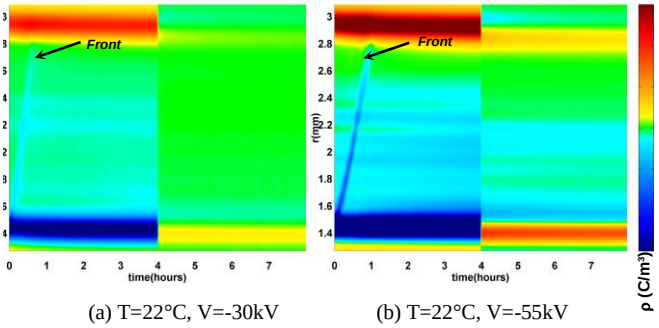

(a) T=22°C, V=-30kV (b) T=22°C, V=-55kV

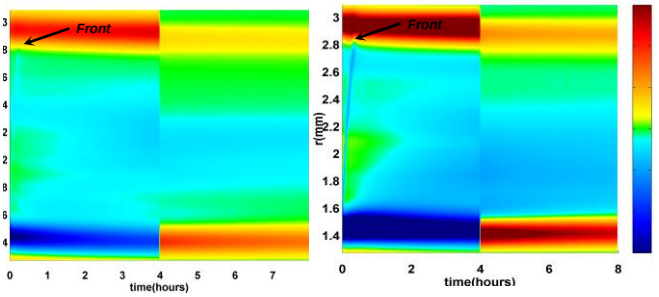

(c) ΔT=10°C, V=-30kV (d) ΔT=10°C, V=-55kV

Fig. 3: Cartographies of space charge density as a function of time along the radius of the insulation in miniature cables obtained at room temperature (a, b) and under thermal gradient of 10°C (60/70°C: c, d) under applied voltage of -30kV (a, c) and -55kV (b, d). The color scale and numbers to the right represent charge density in C/m³ (same for all plots).

geometry the sign of the electric field is the same as that of the polarity of the conductor, it can be deduced from Eq.3 that a negative voltage applied to the conductor leads to a negative space charge in the bulk of the insulation. These features are observed in the space charge patterns reported in Fig.3: Increasing the voltage leads to an increase in the negative bulk space charge, owing presumably to the increase in non-linearity, and imposing a temperature gradient leads also to more space charge as variations in activity are in general more sensible in temperature than in electric field.

2) Negative charge packet.

The second feature, i.e. the front of negative charges is appealing: on the one hand, the charge front is relatively sharp; on the other the transit time of the charge front increases when increasing the stress, which appears as a rather uncommon phenomenon. The front of negative charges is somewhat less intense when increasing temperature; however, it is still clearly visible. The transit time is shorter than that at room temperature, but again, it is shorter for the highest stress. Such features could be repeatedly measured on different cable sections of the same source. The magnitude of the charge front is about 1C/m³ and its width at half-maximum about 150µm for data of Fig. 3b, representing a field variation of the order of 3.5kV/mm across the charge packet.

In order to depict in some more detail the features of the charge front we have plotted in Fig. 4 the position of the packet of charges as it crosses the insulation, considering space charge data obtained at room temperature. The decrease of the velocity of the front with increasing the stress is evident. In order to

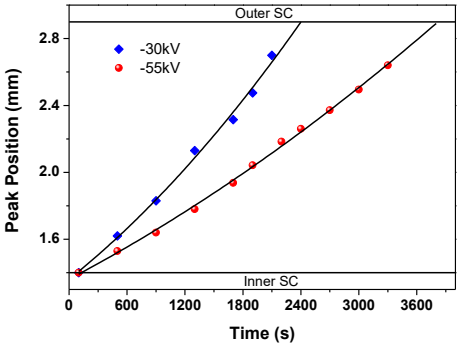

(a) Position of the front as a function of time and fit to a polynomial function.

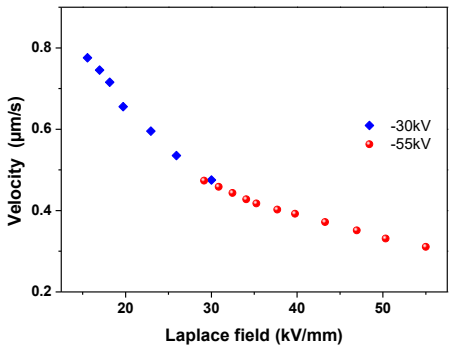

(b) Velocity of the charge front as a function of the Laplace field

Fig. 4: Position of the charge front and velocity of the front as a function of time and field as obtained from data of Fig.3.a) and 3.b).

analyze the propagation of the front, we have plotted in Fig.4b the velocity of the charge packet obtained from derivation of fitted data of Fig. 4.a. as a function of the Laplace field defined as:

$$E(r) = \frac{V_a}{r \times \ln(r_3/r_2)} \qquad (4)$$

where V_a is the applied voltage to the conductor. One remarkable feature is that the data in Fig. 4b at 30 kV and 55 kV overlap and provide consistent values when the field at the inner conductor at 30 kV is similar to that at the outer conductor at 55 kV. Actually, it must be stressed that the field distribution is no longer exactly the capacitive field distribution as space charge already settles in the first hour of stressing, grading the field. The above results show an apparent negative differential mobility (NDM) of carriers [10], i.e. a decrease of the mobility with increasing the field. Interestingly, Chen et al. [11] reported such process for positive carriers when carrying out space charge measurements when applying voltage pulses under a constant DC field. The reported effect was in the same field range as applied herein. NDM is also one of the processes explaining the propagation of charge packets maintaining their shape [5]. Therefore, the propagation of the charge front with maintaining the charge front is already an indication of a NDM. Other reports dealing with negative differential mobility for holes in polyethylene can be found; however, to our knowledge, this seems to be the first evidence for negative carriers.

Cite as: T.T.N. Vu, G. Teyssedre, B. Vissouvanadin, C. Laurent, "*Charge front and negative differential mobility in HVDC model cables*", IEEE Int. Conf. on Electrical Insulation and Dielectric Phenomena (CEIDP), Ann Arbor, MI, USA, 18-21 Oct. 2015. Proc. CEIDP, pp. 19-22, **2015**. DOI: 10.1109/CEIDP.2015.7352104

B. *Current transients*

Figure 5 shows charging current transients obtained on mini-cable sample at 40°C under different fields. For almost all temperature values, the charging current increases at short time and reaches a maximum value, then it decreases with time for approaching steady state value. Moreover, the involved mechanism is clearly thermally activated since the time to peak decreases with increasing temperature, following approximately an Arrhenius law (see Fig. 5.b).

There are at least three processes to consider for explaining such an increase of the transient current during short time:

1) Charges injection and transport through the insulation – with time-to-peak directly related to the transit time of carriers through the insulation;

2) A process linked only to the front of negative charges previously observed on space charge patterns. The time to current peak could be related to the transit of charge front;

3) An association of field dependent conductivity and divergent field (due to cylindrical geometry) with a current transient due to balancing of the field distribution.

Hypothesis 3) above has been checked by obtaining a conduction equation function of field and temperature and computing the transient current. No current rise was predicted, discarding this possibility [12]. In regards to Case 2), we have plotted in Fig. 5.b) the time to current peak as a function of temperature for some voltage values. With extrapolation to room temperature, consistent values of the transit time from space charge and current are obtained (about 2000s for -30kV stress). However, the extrapolation fails for the trends regarding field dependence for fields under 30kV/mm, along with the high temperature case (60-70°C) where the transit time in PEA is much larger than in current. Hence, though more data would be necessary with changing polarity for example, transient processes in space charge and current do not appear correlated in an evident way. Finally, it is worth stressing on the potential harmfulness of such space charge transient processes for cables endurance [6]. Kinetic energy and field strengthening are among the harmful processes whereby early ageing and breakdown of insulations may occur.

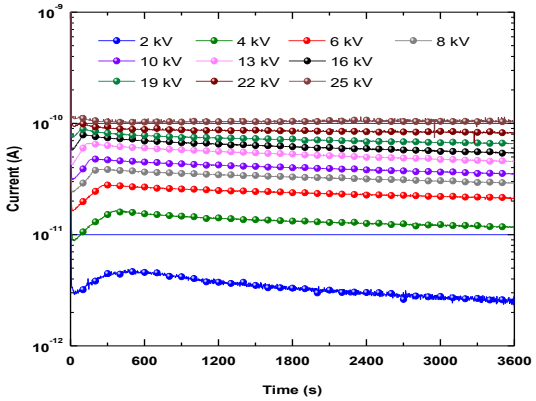

(a) Charging current transient at 40°C

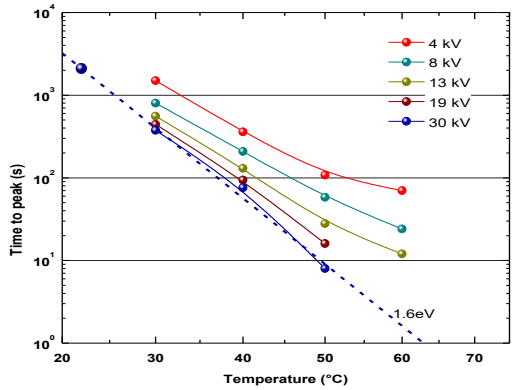

(b) Arrhenius plot of time to peak vs. applied voltage and temperature.

Fig. 5: Charging current transient of mini-cable for different applied voltages and time to current peak function of temperature and field.

IV. CONCLUSION

Space charge measurements were realized on miniature cables at room temperature or under temperature gradient, and considering different stresses. Homogeneous negative space charge build-up was observed in the bulk of the insulation, consistently with what is expected from a field and temperature dependent conductivity material with a negative voltage applied to the cable conductor. In addition, a single space charge packet was observed to form at voltage application, crossing the insulation. It features negative differential mobility of negative charges with a packet velocity decreasing with increasing field. No evident correlation to current transients could be produced.

REFERENCES

[1] J.M. Alison, "A high field pulsed electro-acoustic apparatus for space charge and external circuit current measurement within solid insulators", Meas. Sci. Technol., vol. 9, pp. 1737-1750, 1998.

[2] D. Fabiani, G.C. Montanari, L.A. Dissado, C. Laurent and G. Teyssedre, "Fast and slow charge packets in polymeric materials under DC stress", IEEE Trans. Dielectr. Electr. Insul., vol. 16, pp. 241-250, 2009.

[3] N. Hozumi, H. Suzuki, T. Okamoto, K. Watanabe and A. Watanabe, "Direct observation of time-dependent space charge profiles in XLPE cable under high electric fields", IEEE Trans. Dielectr. Electr. Insul., vol. 1, pp. 1068-1076, 1994.

[4] A. See, L. A. Dissado and J. C. Fothergill, "Electric field criteria for charge packet formation and movement in XLPE", IEEE Trans. Dielectr. Electr. Insul., vol. 8, pp. 859-866, 2007.

[5] F. Baudoin, C. Laurent, G. Teyssedre and S. Le Roy, "Charge packets modeling in polyethylene", Appl. Phys. Lett., vol. 104, p. 152901, 2014.

[6] G.C. Montanari, "Bringing an insulation to failure", IEEE Trans. Dielectr. Electr. Insul., vol. 18, pp. 339-364, 2011.

[7] B. Vissouvanadin, T.T.N. Vu, L. Berquez, S. Le Roy, G. Teyssedre and C. Laurent, "Deconvolution techniques for space charge recovery using pulsed electroacoustic method in coaxial geometry," IEEE Trans. Dielectr. Electr. Insul., vol. 21, pp. 821-828, 2014.

[8] D. Fabiani et al., "HVDC cable design and space charge accumulation. Part 3: Effect of temperature gradient". IEEE Electr. Insul. Mag., vol. 24_2, pp. 5-14, 2008.

[9] H. Ghorbani, M. Jeroense, C.O. Olsson and M. Saltzer, "HVDC cable systems—Highlighting extruded technology", IEEE Trans. Power Deliv., vol. 29, pp. 414-421, 2014.

[10] J. P. Jones, J. P. Llewellyn and T. J. Lewis, "The contribution of field-induced morphological change to the electrical aging and breakdown of polyethylene", IEEE Trans. Diel. Electr. Insul, vol. 12, pp. 951-966, 2005

[11] G. Chen and J. Zhao, "Observation of negative differential mobility and charge packet in polyethylene", J. Phys. D: Appl. Phys., vol. 44, p. 212001, 2011.

[12] T.T.N. Vu, G. Teyssedre, B. Vissouvanadin, J.Y. Steven and C. Laurent, "Transient space charge phenomena in HVDC model cables", Proc. 9th Intern. Conf. Power Cables, Versailles, France, June 2015, pp. 1-6.

Cite as: T.T.N. Vu, G. Teyssedre, B. Vissouvanadin, C. Laurent, "*Charge front and negative differential mobility in HVDC model cables*", IEEE Int. Conf. on Electrical Insulation and Dielectric Phenomena (CEIDP), Ann Arbor, MI, USA, 18-21 Oct. 2015. Proc. CEIDP, pp. 19-22, **2015**. DOI: 10.1109/CEIDP.2015.7352104